Journal of Chemical Reviews, 2021, Volume 3, Issue 1, pages 40-49

Focus Review Article

Voltage Stability of Wind Turbines Equipped with DFIG Based on PID-Based Control Method

Ebadollah Amouzad Mahdiraji[1*], Amir Yousefi Talouki[1]

[1] *Department of Engineering, Sari Branch, Islamic Azad University, Sari, Iran*

Receive Date: 30 March 2020 **Revise Date:** 03 July 2020 **Accept Date:** 29 October 2020

Abstract

With the new structural changes of power system that has emerged in recent years, which makes manufacturing units transmit more and more electrical power from the transmission lines. It is expected that a wider voltage collapse in the power systems will happen. In this research study, a new PID-based control method was used, providing a PCC-voltage feedback control to increase the reactive power from the wind-turbine equipped with a doubly-fed induction generator (DFIG) at high voltage drop. The proposed method is an improved control scheme for the voltage collapse, by which a part of the wind energy, causing a network failure that is temporarily stored in the rotor energy and the remained energy is kept until DC voltage and rotor current are in the hazardous parts. The purpose of the rotor side controller is to independently determine the stator active and reactive the power, which the control of the reactive power using the rotor side converter can cause the stator voltage to remain constant in the desired range. The accuracy and performance of the proposed method were confirmed by simulating a typical power system, in the MATLAB/SIMULINK environment.

Keywords: Power quality; Power system stability; Wind power plant; Double-fed induction generator

Graphical Abstract

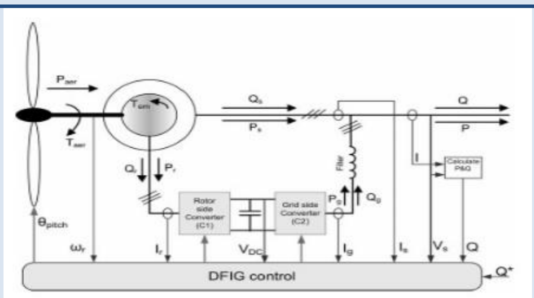

Ebadollah Amouzad Mahdiraji

Ebadollah Amouzad Mahdiraji completed his bachelor's and master's degrees in power electrical engineering at the Islamic Azad University of Sari Branch in 2013 and 2015. Respectively, he is currently a researcher in the field of energy and power systems. His research areas of interest include transient's analysis in electrical equipment, optimization, and operation of smart grids.

Amir Yousefi Talouki

Amir Yousefi Talouki completed his bachelor's and master's degrees in power electrical engineering at Sari Branch of the Islamic Azad University in 2011 and 2016. Respectively, he is currently a researcher in the field of energy and power systems. His research areas of interest include transient's analysis in electrical equipment, protection, and operation of micro-grids.

*Corresponding author: ebad.amouzad@gmail.com

Introduction

With the development of the environmental concerns and energy saving strategies in exploiting renewable energy sources, wind power usage has been increasing in many countries all over the world as compared to other energy sources. The use of wind turbine technologies is a good choice compared to other renewable energy sources since it does not require water, no environment pollution is engaged, no fuel is needed. It also creates a sustainable energy system [1-3]. In the last two decades, the wind energy conversion technologies have undergone a lot of change. The development and growth of wind energy have begun with the low-cost energy acquisition with high efficacy and high reliability, gaining better power and better network connectivity and public acceptance [4-7]. In the wind turbine system, the generator converts the rotational power of the wind turbine into electricity. In wind system, the generator plays an important role and different generators have various performances in interacting with the network. Today, three types of wind turbines (Squirrel Cage Induction Generators, Doubly-fed induction generator, and direct-driven synchronous generator) are commonly used around the world [8-11]. In DFIGs, a voltage converter is used to feed the rotor wiring. The stator wiring is connected to the network and rotor wiring of the voltage converter and the other side of the voltage converter is connected to the network. This converter separates the frequency of the electric network and the mechanical frequency of the rotor. As a result, it allows the wind turbines to operate at different speeds. This converter has a control loop that allows the wind turbines to be controlled continuously [12-15]. According to [16] and [17], the purpose of stability in the power system is to maintain a balance between the power production and consumption during normal conditions, as well as the return to an acceptable equilibrium point in the post-turbulence conditions. In this regard, power system stability, according to the system response is categorized as the rotor angle stability, frequency stability, and voltage stability [18-21]. Wind turbines are not synchronously connected to the power grid and therefore do not participate in oscillating electromechanical mode.

On the other hand, these devices also do not apply a new oscillating mode to the power system because their generator technology is ineffective in the power system oscillations [22-25]. In this work, an improved control scheme of voltage collapse was provided to temporarily store a part of the wind energy that causes a network failure and the remained energy is maintained until DC voltage and rotor current are in the hazardous part [26-28]. In addition, the results of the comparison of the performance of the model and the control system were explored in the short-circuit fault mode in the network.

Controlling a System Equipped with DFIG

DFIG control involves controlling the rotor side and grid side converters. The purpose of independently controlling the rotor side is to regulate the active and reactive powers of the stator [29-31].

Active power control using the rotor side converter can cause the stator voltage to remain stable within the desired range when the DFIG feeds into a weak power network that is without local reactive power compensator. In the stator flux reference apparatus, the relation between translator and dp-axis voltages, currents and fluxes are as follows, by placing the d-axis in the direction of the stator flux we have:

$$\lambda_s = \lambda_{ds} = L_s i_{ds} + L_m i_{dr} \tag{1}$$

$$\lambda_{qs} = 0 \tag{2}$$

$$i_{qs} = -\frac{L_m}{L_{is} + L_m} i_{qr} \tag{3}$$

Having substituted the relation (3) in (1), we have:

$$T_e = -\frac{3}{2}\frac{P}{2}\,\frac{L_m}{L_{is} + L_m}\lambda_{ds} i_{qr} \tag{4}$$

Because the inductance matrix is not in the diagonal stator flux reference, any change in voltage components d or q causes a change in both components of the current [32-35].

To solve the problem, the equations must be compensated for the corresponding values (V_{dr}). First, we define a parameter called the induction motor friction coefficient:

$$\sigma = 1 - \frac{L_m^2}{(L_{is} + L_m)(L_{ir} + L_m)} \tag{5}$$

Based on the (3), we have:

$$\lambda_{dr} = 1 - \frac{L_m^2}{L_m + L_{is}}\lambda_{ds} + \sigma(L_{ir} + L_m) i_{dr} \tag{6}$$

$$\lambda_{dr} = \sigma(L_{ir} + L_m) i_{qr} \tag{7}$$

(8)

$$V_{dr} = r_r i_{dr} + \sigma(L_{is} + L_m) - \frac{di_{qr}}{dr} - s\omega_s \sigma \frac{di_{dr}}{dt}(L_{ir} + L_m) i_{qr}$$

(9)

$$V_{dr} = r_r i_{dr} + \sigma(L_{is} + L_m) - \frac{di_{qr}}{dr} - s\omega_s \sigma (L_m i_{ms} + \sigma L_r i_{dr})$$

The stator flux angle is calculated from the following equation:

(10)

$$\lambda_{as} = \int (V_{as} - R_s i_{as}) dt$$

(11)

$$\lambda_{\beta s} = \int (V_{\beta s} - R_s i_{\beta s}) dt$$

(12)

$$\theta_s = \tan^{-1} \frac{\lambda \beta_s}{\lambda_{as}}$$

where the λas and $V\beta s$,as well as ias and $i\beta s$ are obtained using the Clarke transformation as follows [36-38]:

(13)

$$f_{a\beta o} = c f_{abc}$$

(14)

$$(fa\beta o)^T = [f_a \, f_\beta \, f_o]$$

(15)

$$c = \frac{2}{3}\begin{bmatrix} 1 & -\frac{1}{2} & -\frac{1}{2} \\ 0 & -\frac{\sqrt{3}}{2} & \frac{\sqrt{3}}{2} \\ \frac{1}{2} & \frac{1}{2} & \frac{1}{2} \end{bmatrix}$$

Power electronic converters are divided into two major categories: Voltage source converters (VSCs) and current source converters (CSC). In this work, VSCs are investigated; high efficiency, low cost, and appropriate physical dimensions are among its features. Their main function is to convert the DC voltage to AC voltage with the given voltage range and frequency. Therefore, the output parameters of the converter can be adjusted with the control strategy and the proper modulation for the inverter switches. Voltage source converters that are connected to the power network are called network-connected converters [39-41].

Suggested Control Strategy

When a fault occurs in the main power network, the common coupling point voltage will drop. In these conditions, we will see undesired transient states in the rotor and stator's structures. The voltage drop in the common bus prevents the proper transfer of active power from the wind turbine to the network [42-45].

This will result in severe DC voltage oscillations. In the asymmetric error condition, the negative-sequence currents of the stator will appear as a magnetic motive force (MMF) in the stator space and clockwise direction. These MMFs produce a magnetic flux in the clockwise direction and in the stator and rotor's spaces. These fluxes will incite electric propulsion with frequency ωs (2-S) in the rotor circuit [46-48]. Therefore, the induced component in the rotor circuit has the frequency $F_s(2\text{-}S)$. With more severe fault on the stator side, the current harmonics in the rotor circuit are increased and thus we will observe the harmonic components in the mechanical torque. In the symmetric error condition, the stator voltage will be suffered a sudden drop. The relationship between the stator voltage and the stator charge is based on the Faraday's law. For each phase will have the following relation.

(16)

$$u_{sj} = r_s i_{sj} + \frac{d\Psi_{sj}}{dt}$$

(17)

$$\Psi_{sj} = \int (u_{sj} - r_s i_{sj}) dt$$

In the above relations, j can be a, b, and c phases. The electric propulsion caused by the stator flux will drop sharply. This sharp drop is presented as a shock waveform. Therefore, the stator flux will have a DC component [49-51].

This DC value will be lost due to the circuit's resistance. The DC flux component that is seen by the rotor has a frequency f_m. The transient DC component in the leakage flux of the electric propulsion force will be induced in the rotor circuit. Therefore, when an error is presented in the network, the rotor current will be high and can damage the power converter [52-55].

Hence, it is necessary to design a proper control strategy for this situation. The control of the rotor's flow to quench the asymmetric component trace of the negative sequence in the stator current as well as DC components will be the symmetric errors. These two components will result in the excessive increase in rotor currents and can cause significant damage to the converters during the operation. The typical RSC control loops along with the proposed system are shown in Figure 1.

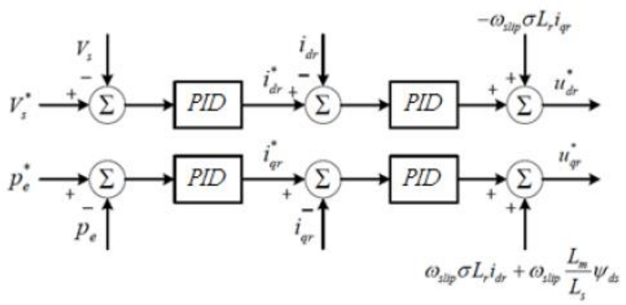

Figure 1. The RSC control loops

In Figure 1, the active output power of the stator or the electromagnetic torque is related to the rotor current in the a-axis and the reactive output power of the stator or the terminal voltage is related to the rotor current in the d-axis. The conventional PID controllers are applied in the external loops to regulate active and reactive power and in the internal circuits to regulate the flow of the rotor. In the proposed control strategy, the dq reference frame rotational speed is assumed to be equal to the synchronous speed [56].

This assumption is also available in steady state. However, during the stator voltage transient modes, the stator flux rotational speed varies with the vector of the spatial voltage.

Therefore, ω is not necessarily equal to the synchronous speed. Given the drop in the network power and its transient states, the model of the DFIG transient state is different, and consequently the control strategy will be different. In the DFIG control plane of rotor side, which uses PID and dual flow regulators, one is used for the positive sequence component and the other for the negative sequence component. It should be noted that up to several low pass filters will be required to detect the DC component corresponding to the negative sequence, positive sequence, and components associated with the stator charge. Of course, the use of filters will result in a delay in the system. Therefore, the system will not be completely decoupled, which will worsen the dynamic response and stability of the system.

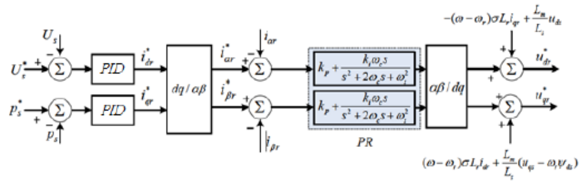

Figure 2. Control of the rotor side converter

Figure 2 compared to the control strategy of Figure 1, the controller gain will be larger. However, the bandwidth of the circuit will be expended by setting the value ofωc. Therefore, it will reduce the sensitivity of the system to the network faults and slow frequency changes. These controllers, which are the function of the PID controller performances for the setting reference values, are applied in the reference frame of $\alpha\beta$. It is obvious that in the stationary reference frame of $\alpha\beta$, the components of the rotor currents in DFIG will be ac components with the frequency $\omega s' - \omega s$. The DC components of the stator flux are also observed as a DC component.

The resonant controller, which has been set in ωs is likely to adjust the positive and negative sequence flows in $\omega s' - \omega s$. It is even possible to provide a steady state error. Therefore, the discussed controlled strategy will properly control the components of the negative and positive sequence without filtering needs.

Examining and Evaluating the Simulated System

The simulated system in this study is demonstrated in Figure 3.

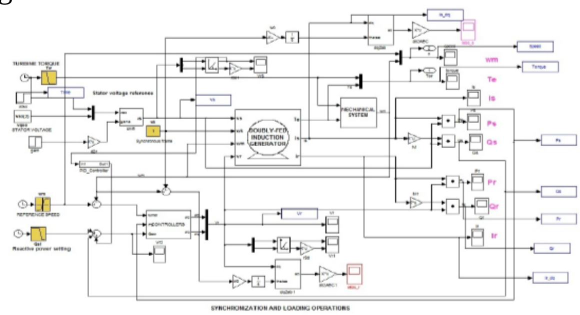

Figure 3. The simulated system.

In the turbines connected to the network, the turbine always tries to work at any speed at its maximum power. Therefore, it is appropriate that the power curve in these turbines always be at the maximum possible extent and also be similar to the speed-power curve. In these curves, the output power per hour of wind is determined with a single rotor speed. Based on these curves, which indicate the optimal energy production path to the nominal (nameplate) production, the turbine must produce a given power for a given velocity so that if the production rate differs from the value of the given reference of the

speed-power curve, the necessary commands will be issued quickly to change the speed of the rotor.
This can be one of the benefits of the double-feed turbines. Figure 4 illustrates the general schema of a DFIG turbine. The applied AC/DC/AC converter in Figure 3 consists of two parts of the network side converter and the rotor side converter that are shown respectively with C_{ROTOR} and C_{GRID}, and these two are designed to control rotor current and voltage in order to separate the network from the rotor.

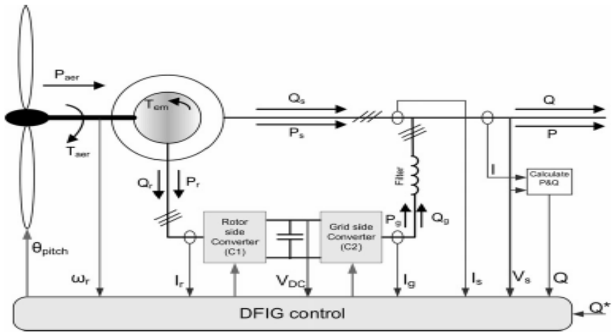

Figure 4. The system consists of a DFIG

The disturbances entered into the system for the change of the reference power of the stator power at t=20s is $\Delta Q = 0.3pu$, the mechanical torque rate obtained from the wind is $\Delta T = -0.5pu$ at the time t=12.5s and the mechanical velocity changes at time t=17s are $\Delta\omega ref = 0.3pu$.
Figure 5 shows the active power consumption in the Wind-DFIG rotor. It was shown that if the controller is not used, the PID will be observed. The amplitude of these oscillations increases over time, which indicates that the system is unstable. It is clearly visible in Figure 6. The Figures 7 and 8 illustrate the active power injection by the stator in DFIG and the electric torque rate, respectively. The electric torque with magnification in the interval t=[15s-30s] is shown in Figure 8. It is clear that lack of using the proposed controller results in a growth in oscillation amplitude of the torque over time. This will result in the system instability. The reactive power exchanged by the DFIG rotor and DFIG stator are represented in Figures 9 and 10, respectively [57-60].
Figure 11 shows that rotor speed changes. The voltage and current components for the stator and the rotor are shown in Figures 11 and 16, respectively.

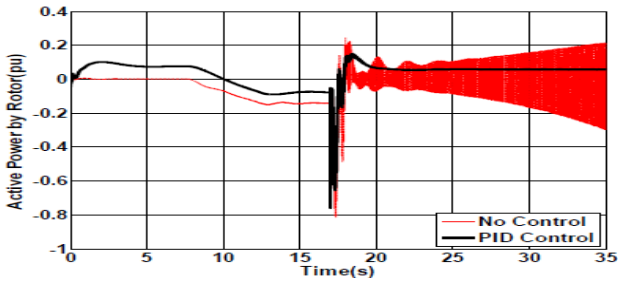

Figure 5. The active power consumption in Wind-DFIG rotor

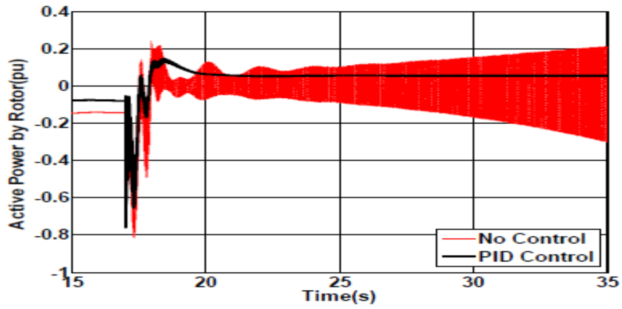

Figure 6. The active power consumption in the Wind-DFIG rotor at magnification range t= [15s-35s]

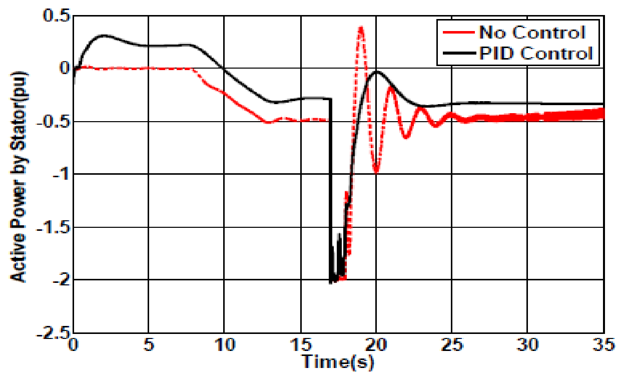

Figure 7. The active power injection by the stator in DFIG

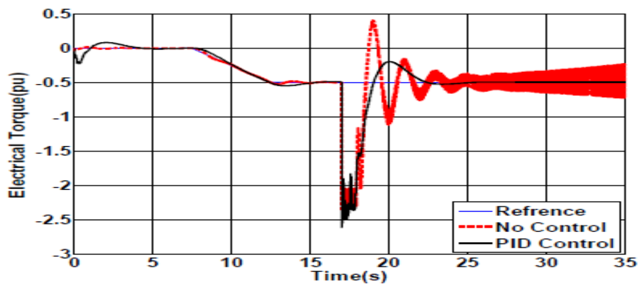

Figure 8. The electrical torque in DFIG

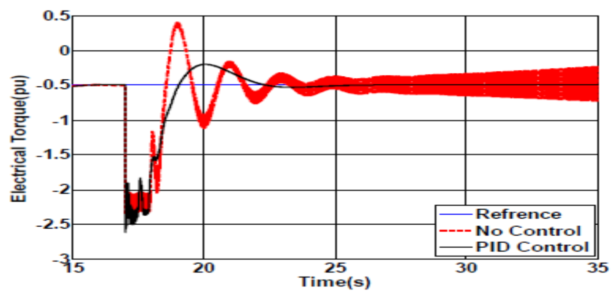

Figure 9. The eclectic torque at magnification range t = [15s-35s]

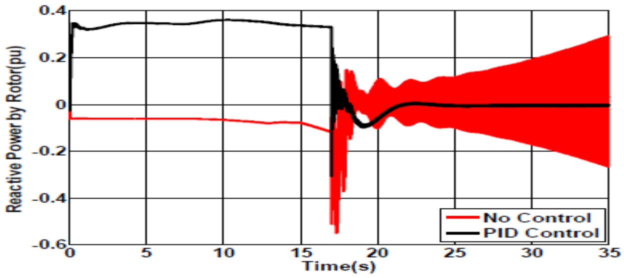

Figure 10. The reactive power exchange by rotor in DFIG

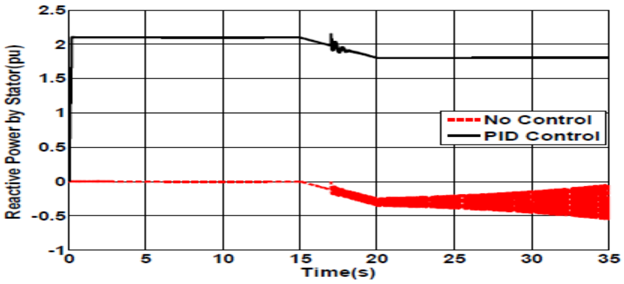

Figure 11. The reactive power exchange by stator in DFIG

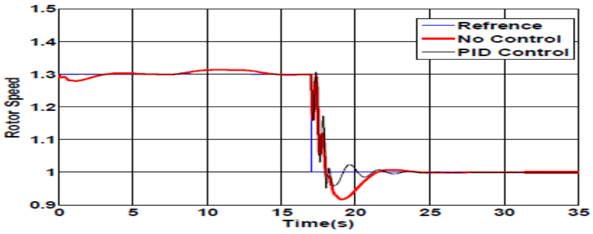

Figure 12. The rotor speed in DFIG

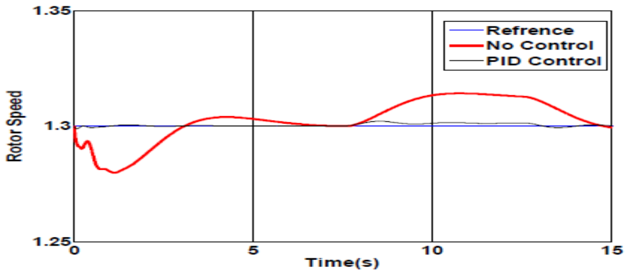

Figure 13. The rotor speed in DFIG at magnification range t=[0s-15s]

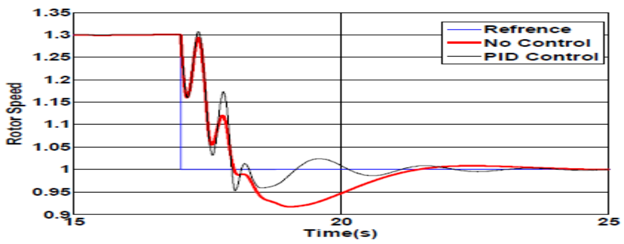

Figure 14. The speed rotor in DFIG at magnification range t=[15s-25s]

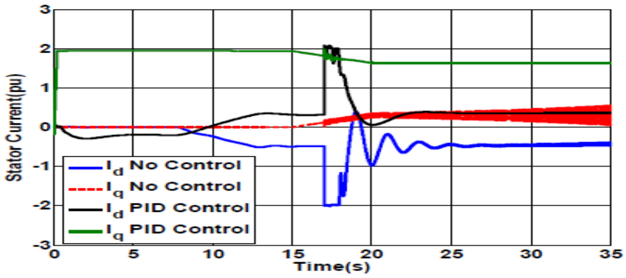

Figure 15. The stator current in DFIG

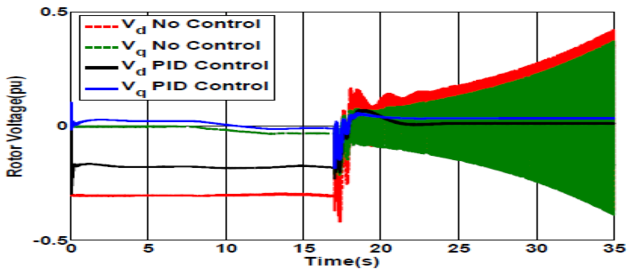

Figure 16. The rotor voltage component in DFIG

In the following section, the dynamic response of the wind turbine with the dual power generator relative to the fault, as well as the effectiveness of the control system in restoring the wind turbine after eliminating the fault to the normal operation prior to the three-phase fault occurrence on the generator terminals are examined.

Given that wind turbines are more influential on the electric power generation and have a high share in the power generation, they should not be disconnected from the network when the fault occurs, because the power network stability can be threatened by a reduction in production. Therefore, the control system should be able to manage the system in such a situation and when the fault has been resolved, returns the wind turbines to its normal state in the shortest possible time.

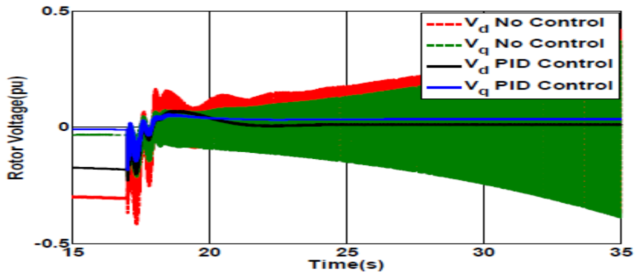

Figure 17. The rotor voltage components at magnification t=[15s-30s]

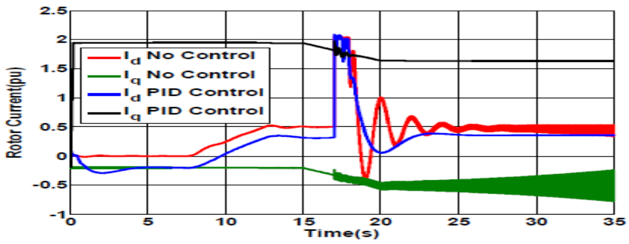

Figure 18. The Rotor current components

If the purpose is to make the wind turbines work in a single power factor, then the reactive power reference value will be zero. In this situation, the value of the generator terminal voltage will not be equal to a per-unit, and the turbines will work in the single power factor; however, the output voltage is not equal to per-unite. Moreover, if the goal is to keep the terminal voltage constant, then it cannot be expected that the reactive power value to be zero. As it is known, keeping the voltage constant is at the expense of the reactive power consumption.

Conclusion

In this work, a variable speed wind turbine was simulated with a doubly fed induction generator and the control system for the wind turbine rotor side converter was proposed to obtain the maximum wind energy. As the simulation results revealed, the introduced control system could control both the active and reactive powers. The proposed control system is also capable of limiting the wind turbine output at high wind speed. The efficacy of the suggested model for the wind turbine and its control system was explored. As the simulation results indicated, the control system used a reactive power compensator to prevent the voltage instability. Finally, a method of combining the wind turbines in a wind power plant was presented in an equivalent wind turbine. The proposed model was accurate enough to correctly model the behavior of the turbines when existing wind turbines receive different wind speeds. The simulation results demonstrated that the replacement of the wind turbines with the aggregation model can model the behavior of the entire wind power plant with sufficient accuracy.

Reference

[1] M. Ramamoorty, M. M. B. Narayanan, and S. Parameswaran *et al.*, Transient performance of grounding grids, *IEEE Trans. Power Del.*, 4(4) (1989), 2053–2059

[2] A. Geri, Behavior of grounding systems excited by high impulse currents: the model and its validation, *IEEE Trans. Power Del.*, 14(3) (1999), 1008–1017

[3] A. F. Otero, J. Cidras, and J. L. del Alamo, Frequency-dependent grounding system calculation by means of a conventional nodal analysis technique, *IEEE Trans. Power Del.*, vol. 14(3) (1999), 873–878

[4] A. P. Meliopoulos and M. G. Moharam, Transient analysis of grounding systems, *IEEE Trans. Power App. Syst.*, PAS-102(2) (1983), 2-19

[5] A. D. Papalexopoulos and A. P. Meliopulos, “Frequency dependent characteristics of grounding systems, *IEEE Trans. Power Del.*, 2(4) (1987), 1073–1081

[6] R**.** Velazquez and D. Mukhedkar, Analytical modelling of grounding electrodes transient behavior,” IEEE Trans**.** Power Apparatus and Systems**,** 103 (1984)**,** 1314-1322.

[7] A. Samimi, S. Zarinabadi, AH. Shahbazi Kootenaei, A. Azimi, M. Mirzaei, Kinetic Overview of Catalytic Reforming Units (Fixed and Continuous Reforming), *Chemical Methodologies*, 4(1) (2020), 852-864

[8] V. Cooray and N. Theethayi, Pulse propagation along transmission lines in the presence of corona and their implication to lightning return strokes, *IEEE Trans. Antennas Propag.*, 56(7) (2008), 1948–1959

[9] H. M. Kudyan and C. H. Shih, A nonlinear circuit model for transmission lines in corona, *IEEE Trans. Power App. Syst.*, PAS-100(3) (1981), 1420–1430

[10] M.Mihailescu-Suliciu and I. Suliciu, A rate type constitutive equation for the description of the corona effect, *IEEE Trans. Power App. Syst.*, PAS-100(8) (1981), 3681–3685

[11] T. H. Thang, Y. Baba, N. Nagaoka, A. Ametani, J. Takami, S. Okabe, and V. A. Rakov, A simplified model of corona discharge on an overhead wire for FDTD computations, *IEEE Trans.* Electromagn. Compat., 54(3) (2012), 585–593

[12] A. Bozorgian, S. Zarinabadi, A. Samimi, Optimization of Well Production by Designing a Core pipe in one of the Southwest oil Wells of Iran, *Journal of Chemical Reviews*, 2(2) (2020), 122-129

[13] T. H. Thang, Y. Baba, N. Nagaoka, A. Ametani, J. Takami, S. Okabe, and V. A. Rakov, FDTD simulation of lightning surges on overhead wires

in the presence of corona discharge, *IEEE Trans.* Electromagn. Compat., 54(6) (2012), 1234–1243

[14] C. de Jesus and M. T. Correia de Barros, Modelling of corona dynamics for surge propagation studies, *IEEE Trans. Power Del.*, 9(3) (1994), 1564–1569

[15] T. Noda, T Ono, H. Matsubara, H. Motoyama, S. Sekioka, and A. Ametani, Charge-voltage curves of surge corona on transmission lines two measurement methods, *IEEE Trans. Power Del.*, 18(1) (2003), 307–314

[16] A. Inoue, Propogation analysis of overvoltage surges with corona based upon charge versus voltage curve, *IEEE Trans. Power App. Syst.*, PAS-104(3) (1985), 655–662

[17] A. Samimi, S. Zarinabadi, AH. Shahbazi Kootenaei, A. Azimi, M. Mirzaei, Corrosion Classification of Pipelines in hydrocracking units by Data Mining, South African Journal of Chemical Engineering, 31 (2020), 44-50

[18] P. S. Maruvada, D. H. Nguyen, and H. Hamadani-Zadeh, Studies on modeling corona attenuation of dynamic overvoltages, *IEEE Trans. Power Del.*, 4(2) (1989), 1441–1449

[19] X. R. Li, O. P.Malik, and Z. Zhao, A practical mathematical model of corona for calculation of transients on transmission lines, *IEEE Trans. Power Del.*, 4(2) (1989), 1145–1152

[20] R. Davis, R. W. E. Cook, and W. G. Standring, The surge corona discharge, *Proc. Inst. Elect. Eng. Monographs*, 108 (1961), 230–239

[21] P. S. Maruvada, H. Menemenlis, and R. Malewski, Corona characteristics of conductor bundles under impulse voltages, *IEEE Trans. Power App. Syst.*, vol. PAS-96(1) (1977), 102–115

[22] G.V. Podporkin and A. D. Sivaev, Lightning impulse corona characteristics of conductors and bundles, *IEEE Trans. Power Del.*, 12(4) (1997), 1842–1847

[23] T. Narita and S. Okabe, Propagation characteristics of lightning surge with corona discharge on UHV designed transmission line, (in Japanese) *Trans. Inst. Elec. Eng. Jpn.*, 122-B(2) (2002), 307–313

[24] C. Sandoval, Evaluation of corona and line models in electromagnetic transients simulation, IEEE Transactions on Power Delivery, 6(6) (1991), 334-342

[25] Grcev L, Popov M. On high-frequency circuit equivalents of a vertical ground rod. *IEEE Transaction on Power Delivery 2005*, 20(2) (2005), 1598–1603.

[26] A. Samimi, S. Zarinabadi, A. Bozorgian, A. Amosoltani, M. Tarkesh, K. Kavousi, Advances of Membrane Technology in Acid Gas Removal in Industries, *Progress in Chemical and Biochemical Research*, 3 (1) (2020), 46-54

[27] Imece A, Durbak D, Elahi H, et al. Modeling guidelines for fast front transients. *IEEE Transaction on Power Delivery 1996*, 11(1) (1996), 493–506.

[28] Grcev L. Modeling of grounding electrodes under lightning currents. *IEEE Transactions on Electromagnetic Compatibility*, 51(3) (2009), 559–571.

[29] J. R. Marti, F. Castellanos, and N. Santiago, Wide-band corona circuit model for transient simulations, IEEE Transactions on Power Systems, 10(4) (1995), 1003-1013

[30] J.T. Hodgkinson, M. Welch, D.R. Spring, Learning the Language of Bacteria. *ACS Chem. Biol*, 2(11) 2007, 715-17.

[31] A. Jayaraman, T.K. Wood, Bacterial quorum sensing: signals, circuits, and implications for biofilms and disease. *Annu. Rev. Biomed. Eng*, 10 2008, 145-67.

[32] M. Manefield, T.B. Rasmussen, M. Henzter, J.B. Andersen, P. Steinberg, S. Kjelleberg, M. Givskov, Halogenated furanones inhibit quorum sensing through accelerated LuxR turnover. *Microbiology*, 148(4) 2002, 1119-27.

[33] A. Samimi, Risk Management in Information Technology, *Progress in Chemical and Biochemical Research*, 3(2) (2020), 130-134

[34] R.P. Ryan, J.M. Dow, Diffusible signals and interspecies communication in bacteria. *Microbiology*, 154(7) 2008, 1845-58.

[35] C.D. Sifri, Quorum sensing: bacteria talk sense. Clin. Infect. Dis, 47(8) 2008, 1070-76.

[36] P. Williams, K. Winzer, W.C. Chan, M. Camara, Look who's talking: communication and quorum sensing in the bacterial world. *Phil. Trans. R. Soc. Lond. B*, 362 2007, 1119–1134.

[37] T. Bjarnsholt, M. Givskov, Quorum sensing inhibitory drugs as next generation antimicrobials: worth the effort? *Curr. Infect. Dis. Rep*, 10(1) 2008, 22-8.

[38] A. Bozorgian, S. Zarinabadi, A. Samimi, Preparation of Xanthan Magnetic Biocompatible Nano-Composite for Removal of Ni^2+ from Aqueous Solution, *Chemical Methodologies*, 4 (4) (2020), 477-493

[39] B. Raffa Robert, R. Iannuzzo Joseph, R. Levine Diana, K. Saeid Kamal, C. Schwartz Rachel, T. Sucic Nicholas, D. Terleckyj Oksana, M. Young Jeffrey, Bacterial communication ("quorum sensing") via ligands and receptors: a novel pharmacologic target for the design of antibiotic drugs. *J. Pharmacol. Exp. Ther*, 312(2) 2005, 417-23.

[40] T.B. Rasmussen, M. Givskov, Quorum-sensing inhibitors as antipathogenic drugs. *Int. J. Med. Microbiol*, 296 (2-3) 2006, 149-61.

[41] B. Rasmussen Thomas, M. Givskov, Quorum sensing inhibitors: a bargain of effects. *Microbiology*, 152 (Pt 4) 2006, 895-904.

[42] A. Bozorgian, S. Zarinabadi, A. Samimi, Preparation of Xanthan Magnetic Biocompatible Nano-Composite for Removal of Ni^2+ from Aqueous Solution, *Chemical Methodologies*, 4 (4) (2020), 477-493

[43] N. Balaban, M. Givskov, T.B. Rasmussen, In Vivo Studies: Inhibiting Biofilm-Associated Bacterial Infections using QSIs. In Control of Biofilm Infections by Signal Manipulation, *Balaban, N. Ed. Springer: Berlin*, 2 2008, 119-29.

[44] M. Hentzer, M. Givskov, L. Eberl, Quorum sensing in biofilms: Gossip in slime city. *Microb. Biofilms*, 1 2004, 118-40.

[45] M.R. Parsek, E.P. Greenberg, Sociomicrobiology: the connections between quorum sensing and biofilms. *Trends Microbiol*, 13 (1) 2005, 27-33.

[46] A. Samimi, S. Zarinabadi, A. Bozorgian, A. Amosoltani, M. Tarkesh, K. Kavousi, Advances of Membrane Technology in Acid Gas Removal in Industries, *Progress in Chemical and Biochemical Research*, 3 (1) (2020), 46-54

[47] A.R. Horswill, P. Stoodley, P.S. Stewart, M.R. Parsek, The effect of the chemical, biological, and physical environment on quorum sensing in structured microbial communities. *Anal. Bioanal. Chem*, 387 (2) 2007, 371-80.

[48] M. Li, N. Ni, H.T. Chou, C.D. Lu, P.C. Tai, B. Wang, Structure-based discovery and experimental verification of novel Al-2 quorum sensing inhibitors against Vibrio harveyi. *Chem Med Chem*, 3 (8) 2008, 1242-49.

[49] J.B. Andersen, A. Heydorn, M. Hentzer, L. Eberl, O. Geisenberger, B.B. Christensen, S. Molin, M. Givskov, gfp-based N-acyl homoserine-lactone sensor systems for detection of bacterial communication. *Appl Environ Microbiol* 67 2001, 575-585.

[50] W. Galloway, J. Hodgkinson, S. Bowden, M. Welch, D. Spring, Quorum Sensing in Gram-Negative Bacteria: Small-Molecule Modulation of AHL and AI-2 Quorum Sensing Pathways. *Chem. Rev*. 111 2011, 28–67.

[51] M.G. Kociolek, Quorum-Sensing Inhibitors and Biofilms. *Anti-Infective Agents in Medicinal Chemistry*, 8 2009, 315-326 315.

[52] R. Smith, B. Iglewski, Pseudomonas aeruginosa quorum-sensing systems and virulence. *Current Opinion in Microbiology*, 6 2003, 56-60.

[53] M. Abdollahbeigi, Optimizing the Process of Di-Isobutyl Phthalate Production Using Vapor Permeation, *DAV International Journal of Science*, 4(2) (2015), 47-52

[54] M.J. Choobineh, B. Nasrollahzadeh, M. Abdollahbeigi, Investigation of Contact Resistance Effect on Finned Pipes under Natural and Forced Convection, *DAV International Journal of Science*, 4(2) (2015), 58-76

[55] B. Nasrollahzadeh, M.J. Choobineh, M. Abdollahbeigi, Investigation of Hydrate Formation Kinetics and Mechanism of Inhibitors Effect, *DAV International Journal of Science*, 4 (2015), 49-56

[56] M. Abdollahbeigi, M.J. Choobineh, B. Nasrollahzadeh, Nano Catalyst, Operation Mechanism and Their Application in Industry, *Australian Journal of International Social Research*, 1(5) (2015), 1-6

[57] M. Abdollahbeigi, M.J. Choobineh, B. Nasrollahzadeh, Investigation of Molecular Structure in Gas Hydrate, *Science road Journal*, 3(12) (2015), 74-79

[58] M.J. Choobineh, M. Abdollahbeigi, B. Nasrollahzadeh, the formation of gas hydrate and the effect of inhibitors on their formation process, *Journal of Fundamental Applied Science* 8(2S) (2016), 1150-1159

[59] A. Samimi, S. Zarinabadi, AH. Shahbazi Kootenaei, A. Azimi, M. Mirzaei, Optimization of Naphtha Hydro-Threating Unit with Continuous Resuscitation Due to the Optimum Temperature of Octanizer Unit Reactors, advanced journal of chemistry section A , 3(2) (2020), 165-180

[60] D. Ren, M. Givskov, T. Ramussen, Quorum-Sensing Inhibitory Compounds. In Control of Biofilm Infections by Signal Manipulation, *Balaban, N. Ed. Springer: Berlin*, 2 2008, 51-77.

How to cite this manuscript: Ebadollah Amouzad Mahdiraji, Amir Yousefi Talouki, Effects of Soil Ionization and Lightning Impulse Corona on Lightning Current Strike, *Journal of Chemical Reviews* (*J. Chem. Rev*.), 2021, 3(1), 348-357. DOI: